INFLUENCE OF TITANIUM AND NIOBIUM ON THE STRENGTH–DUCTILITY–HOLE EXPANSION RATIO BALANCE OF HOT-ROLLED LOW-CARBON HIGH-STRENGTH STEEL SHEETS

K. Kamibayashi, Y. Tanabe, Y. Takemoto, I. Shimizu and T. Senuma

Graduate School for Nature Science
Okayama University, Okayama 700-8530 Japan

Abstract

It has been demonstrated that the demand for high strength sheet steels with excellent balances of strength, ductility and hole expansion ratio could be met by steels with a ferrite or bainitic-ferrite matrix strengthened by a large amount of finely dispersed precipitates. In this study, the influence of the precipitation forming elements, Ti and Nb on the balance of strength, ductility and hole expansion ratio has been investigated. Individually, neither Ti nor Nb produces optimum performance but it has been proposed that a carefully selected balance of added Ti and Nb can succeed in meeting the desired combination of properties. The reasons why the individual elements, when used alone, produce inferior performance is explored and the role of sulphides and the formation of textural colonies are both highlighted as playing important roles. Titanium alone can go part way towards satisfying the property demands whilst this has been shown to be more difficult with niobium as a single alloying addition. These observations are thoroughly discussed and explained.

Introduction

A remarkable number of high-strength steels have been developed and used in practice to reduce automotive body weight. Improvement in formability is one of the most important research items in the development of modern high-strength steels. Successful developments of advanced high-strength steels with a good strength−ductility balance are DP and TRIP steels [1,2]. The hole expandability of these steels is, however, poor. On the other hand, bainite or tempered martensite steels show excellent strength–hole expansion ratio balances but their ductility is low. In recent research and development, a large effort has been made to develop steels with a good strength–ductility–hole expansion ratio balance [3-13]. A newly developed steel of this kind consists of a ferrite matrix strengthened by a large amount of finely dispersed precipitates [5-8]. Funakawa and his co-workers [14] investigated the precipitation behavior of these kinds of steels containing Ti, Nb and Mo, and reported the occurrence of interphase precipitation. They also reported the mechanical properties of the steels developed. The influence of the separate or combined addition of Ti, Nb and Mo on the strength–ductility–hole expansion ratio balance was, however, not investigated in detail.

In this study, the influence of the addition of Ti and Nb on the strength–ductility–hole expansion ratio balance of the 600 MPa class steels consisting of a ferrite matrix strengthened by a large amount of precipitates has been investigated.

At first, an experiment was carried out using a Ti and a Nb-bearing steel. The microstructure and texture, the condition of the pierced surface, the behavior of crack initiation and propagation during hole expansion, precipitates and inclusions, etc., were studied in the two steels. By comparing the obtained results from both steels, the main factors influencing the ductility–hole expansion ratio balance were discussed and clarified. The discussion indicated that there exists an optimum ratio of Ti/Nb addition, and to determine this, an additional experiment was carried out using steels with various ratios of Ti and Nb additions.

Finally, we propose an adequate combination of Ti and Nb addition to produce steel with a good ductility–hole expansion ratio balance.

Experimental Conditions

Table I shows the chemical composition of the steels used in the experiment. The chemical composition was designed to obtain a tensile strength of around 600 MPa and a microstructure consisting of a ferrite matrix strengthened by finely dispersed precipitates. The Ti or Nb content of these steels are designed to almost fulfil stoichiometry with C, to avoid the formation of pearlite and grain boundary cementite that lower the hole expandability.

Table I. Chemical Composition of the Steels Used in the Experiment (wt%)

Steel	C	Si	Mn	P	S	Al	Nb	Ti	N
Ti	0.033	0.1	1.49	0.01	0.0062	0.037	-	0.12	0.0018
Nb	0.028	0.1	1.48	0.01	0.0053	0.037	0.22	-	0.0018

The steels were melted in a vacuum furnace and then cast into 50 kg ingots. Figure 1 shows the thermal history of the hot-rolling process. Ingots of 110 mm thickness were reheated at 1250 °C for 60 min for the solution treatment and subsequently hot-rolled at a finishing temperature around 930 °C according to a reduction schedule of: $110 \rightarrow 80 \rightarrow 60 \rightarrow 45 \rightarrow 30 \rightarrow 15 \rightarrow 8 \rightarrow 4.5 \rightarrow 2.8$ mm. The coiling process was simulated using an electrical furnace kept at a temperature of 600 °C, in which the hot-rolled sheets were held directly after hot-rolling for 60 min without a temperature drop below the furnace temperature and then cooled in air.
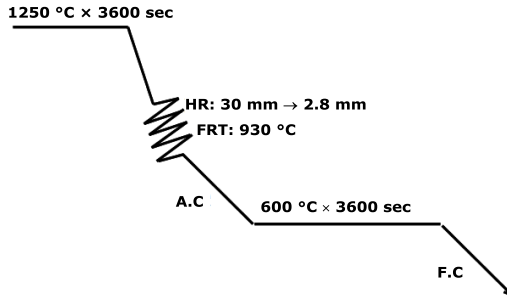
Figure 1. Thermal history of the hot-rolling process.

The microstructure was characterized using optical microscopy (OM), field emission scanning electron microscopy (FE-SEM) and transmission electron microscopy (TEM). The grain size of ferrite and the size of dimples observed on the pierced surface were analysed with an image analysis device (IAD). The texture of the steels was measured and analysed using electron backscatter diffraction patterns (EBSP). The calculation of the r-value from EBSP data was carried out using self-developed software. The chemical composition of precipitates was determined using energy dispersive X-ray (EDX) spectroscopy mounted on the TEM.

The hardness was measured on a micro-Vickers tester with a load of 2.94 N. Each plotted point is an average value of five measurements. Tensile tests and hole expansion tests were carried out to determine the mechanical properties of the steels. The tensile test was performed only in the rolling direction. A Charpy impact test was also carried out in both the rolling and the transverse directions. The test piece of the Charpy impact test consisted of two hot bands glued to each other.

The hole expansion test was performed according to the Japan Federation of Iron and Steel Standard (JFS T1001). The hole was pierced by a 10-mm-diameter punch. The clearance was 12%. For the hole expansion test, an Erichsen testing machine was used. The burred surface was facing upwards. The hole expansion was performed by moving a vertical conic punch of 60° angle upwards. Figure 2 shows schematic diagrams of the devices used for piercing and hole expansion.
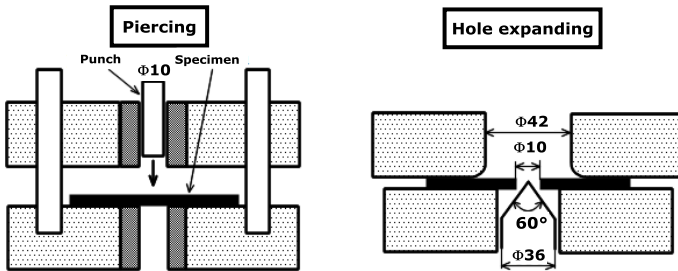
Figure 2. Schematic diagrams of the devices used for piercing and hole expanding.

The hole expansion ratio was calculated by Equation 1. Here, d_0 is the initial diameter of the hole and d is the diameter of the hole expanded so far as a through-thickness crack is just observed. To investigate the propagation behavior of cracks during hole expansion, specimens with hole expansion ratios of 20%, 40% and 70% were produced.

$$\lambda = \frac{d - d_0}{d_0} x100\% \tag{1}$$

Experimental Results

Figure 3 shows the mechanical properties of the Ti and Nb steels. TSxElxλ is a quantity used for evaluating the strength–ductility–hole expansion ratio balance. (A high value of this quantity means a good strength–ductility–hole expansion ratio balance.) It is clearly seen that the strength–ductility–hole expansion ratio balance of the Ti steel is superior to that of the Nb steel.

Table II shows the impact energy determined by the Charpy impact test at a temperature of 22 °C. The difference in impact energy between specimens L, whose notch was perpendicular to the rolling direction, and specimens C, whose notch was parallel to the rolling direction, was larger in the Nb steel than in the Ti steel. Specimen L of the Nb steel had the highest value of impact energy of the four cases, but Specimen C had the lowest. To clarify the reason for the superiority of the ductility–hole expansion ratio balance in the Ti steel, we investigated the microstructure, the condition of the pierced surface, the evolution of cracks during hole expanding, etc.
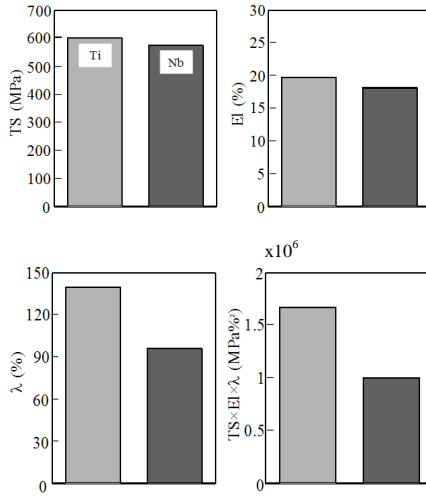
Figure 3. Mechanical properties of Ti and Nb steels.

Table II. Impact Energy Determined by Charpy Impact Test at a Temperature of 22 °C

	Impact energy (J/cm^2)
Ti steel specimen L	171
Ti steel specimen C	161
Nb steel specimen L	209
Nb steel specimen C	138

Figure 4 shows the pierced surface after the hole expansion test. As for the Ti steel, many cracks were observed over the entire circumference. On the other hand, the number of cracks in the Nb steel was limited, and the penetration crack always propagated parallel to the rolling direction. Figure 5 shows the evolution of the surface morphology during hole expansion. As for the Ti steel, many fine cracks were observed in the outer fractured surface of the hole expanded to $\lambda = 20\%$. These cracks reached the boundary between the sheared and fractured surfaces at $\lambda = 40\%$. As the expansion ratio increased to 70%, the number of cracks increased, but none of them propagated inside the sheared zone.
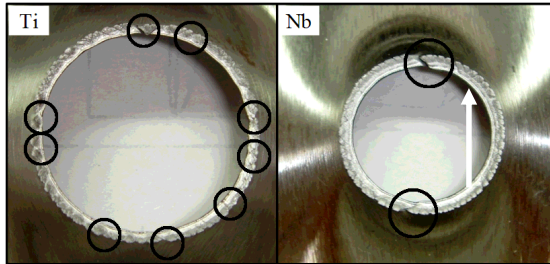
Figure 4. Pierced surfaces after the hole expansion test of Ti and Nb steels.
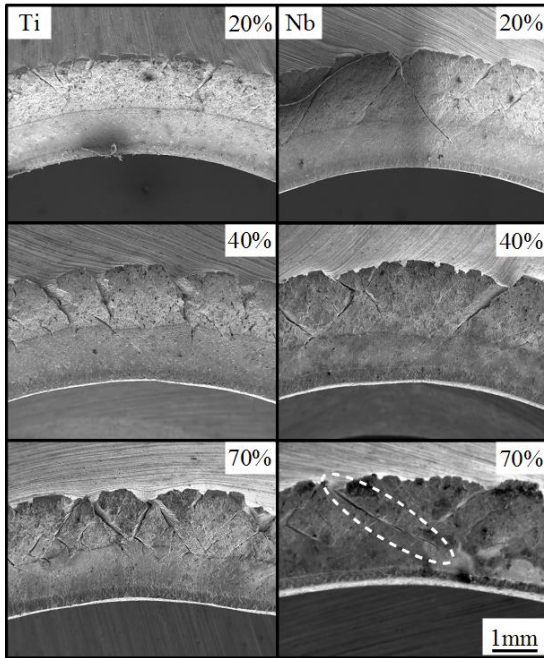(The arrow shows the rolling direction).

Figure 5. Evolution of morphology of the pierced surface during the hole expansion test.

At $\lambda = 20\%$, the number of micro-cracks in the Nb steel was smaller than in the Ti steel, but some of them reached the boundary between the sheared and fractured surfaces. At $\lambda = 70\%$, some cracks penetrating the sheared surface were observed in the Nb steel. It was also observed that the thickness of the pierced surface of the Ti steel was markedly reduced by hole expansion, and the change in the thickness of the Nb steel was not apparent. Thickness reduction in the Ti steel was realized by large numbers of cracks distributed over the entire circumference.

It is well known that the state of the pierced surface markedly affects the hole expansion ratio. The state of the pierced surface is characterized by the ratio of the sheared to fractured surface areas, the numbers and size of micro-cracks and dimples in the fractured surface, and work hardening in the vicinity of the pierced surface.

Figure 6 shows the pierced surface of the Ti and Nb steels. The ratio of the sheared to fractured areas was 56:39 for the Ti steel and 46:49 for the Nb steel. The increase in the ratio of the fractured areas seems to lower hole expandability.

If the vicinity of the pierced surface is significantly hardened by piercing, the hole expansion ratio may be lowered, and therefore the hardness in the vicinity of the pierced surface was measured. Figure 7 shows the hardness distribution up to 2 mm from the surface at three different positions, namely the centre of the sheared area, the centre of the fractured area and the boundary between the sheared and fractured areas. The increase in hardness in the sheared area was lower than in the fractured and boundary areas. The work hardening in the Nb steel was slightly less than that in the Ti steel. Because a higher hardness in the vicinity of a pierced surface is supposed to result in a lower hole expansion ratio, the work hardening behavior cannot explain the inferior ductility–hole expansion ratio balance in the Nb steel.
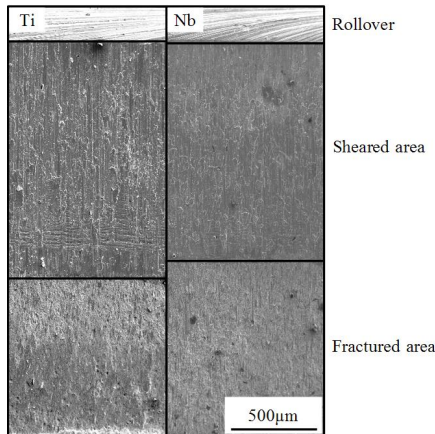

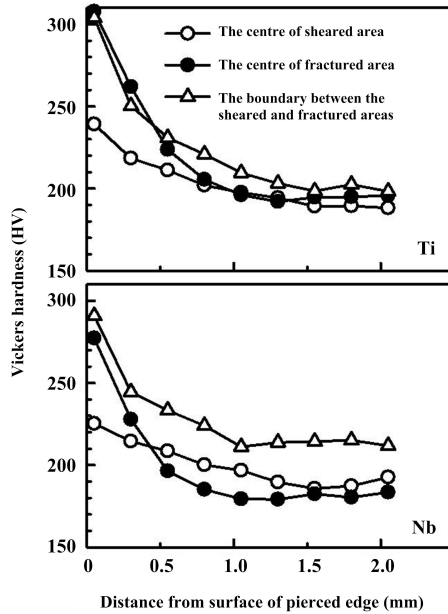Figure 6. Appearance of the surfaces pierced by punch.

Figure 7. Hardness distribution up to 2 mm from the surface at three different positions.

Figure 8 shows the SEM pictures of fractured surfaces of both steels. To quantify the surface condition, the numbers and size of dimples were measured. The mean diameter and standard deviation of dimples observed were 3.62 and 2.45 μm, respectively, in the Nb steel and 2.31 and 1.24 μm, respectively, in the Ti steel. For the latter, 70% of the dimples were between 1.07 and 3.55 μm and the largest dimple size was around 6 μm, whereas 70% of the dimples in the Nb steel were between 1.17 and 6.07 μm and the largest size was more than 11 μm. Both the size and standard deviation of dimples in the Nb steel were clearly larger than those in the Ti steel.
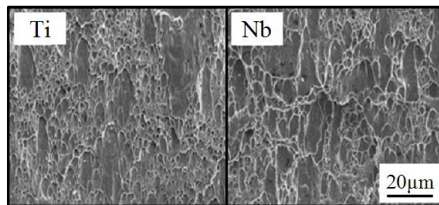

Figure 8. SEM micrographs of the fractured surfaces of the punched hole.

216

Figure 9 shows a cross section of the vicinity of the pierced surface. A number of micro-voids were observed. The number, average size and standard deviation of micro-voids observed in the cross section area in the vicinity of the fractured surface of a representative area of 100 μm x 30 μm of the Ti steel were 87, 1.4 μm and 1.6 μm, respectively, whereas those of the Nb steel were 45, 2.9 μm and 3.3 μm, respectively. The fact that the Ti steel has more micro-voids than Nb steel may relate to the fact that, as shown in Figure 4, in the initial stage of hole expansion more cracks were observed in the Ti steel than in the Nb steel. The fact that the micro-voids in the Nb steel were larger than in the Ti steel may also relate to the fact that the propagation rate of through-thickness cracks in the Nb steel was higher than in the Ti steel.
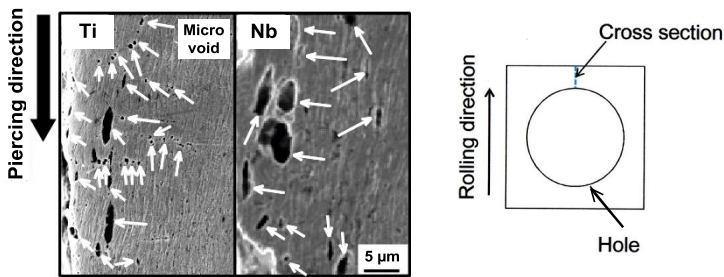

Figure 9. Micro-voids observed in the vicinity of the pierced surface.
The cross section is parallel to the rolling direction.

To examine whether the lower hole expansion ratio of the Nb steel could be mainly attributed to the state of the pierced surface, an additional hole expansion test was carried out using the specimens with a hole machined by electric discharged wire cutting. Although the hole expansion ratio of the machined holes of the Nb and Ti steels increased markedly to 187% and 205%, respectively, a clear difference still remained between the two steels.

To clarify this difference, the microstructures of the two steels were examined, Figure 10. The microstructure of the Nb steel was finer than that of the Ti steel. The average ferrite grain size of the Nb and Ti steels was 2.27 and 3.37 μm, respectively. It was also observed that the microstructure of the Nb steel was more heterogeneous than that of the Ti steel. This heterogeneity was probably caused by partial recrystallization of austenite because of the strong retardation effect of Nb on recrystallization. It is well known that heterogeneity of microstructure is detrimental to the hole expansion ratio.
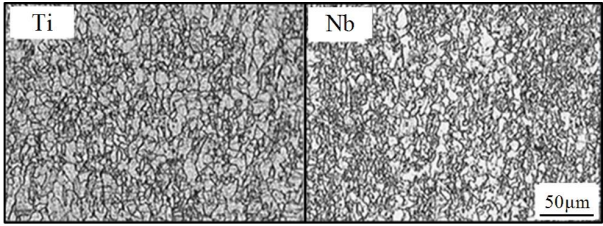
Figure 10. Microstructures of Ti and Nb steels.

To examine the microstructural heterogeneity in detail, a micro-scale textural analysis was carried out. Figure 11 shows the crystal orientations measured in the Ti and Nb steels by EBSP. The ellipses in the Nb steel indicate the presence of colonies (aggregates of grains with similar orientations), which is evidence for the microstructural heterogeneity of the Nb steel.
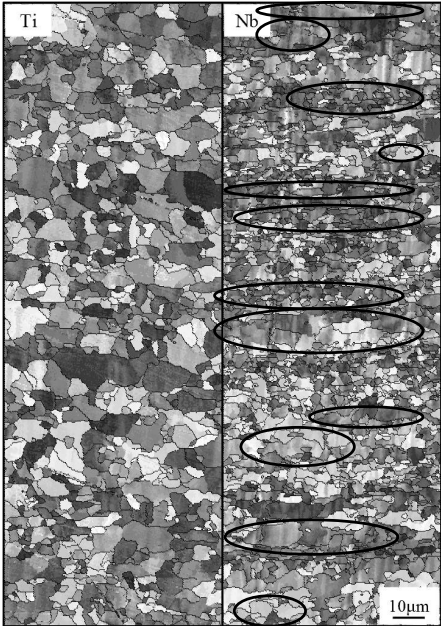

Figure 11. ND crystal orientation maps of Ti and Nb steels.

The hole expansion ratio is also affected by the planar anisotropy of the texture [15]. Figure 12 shows the planar anisotropy of r-values calculated using the orientation distribution function (ODF) data obtained by EBSP measurements at mid-thickness. It is recognized that the Ti steel had a larger planar anisotropy of r-values and a higher average r-value than the Nb steel. Phillips et al. reported that the hole expansion ratio was chiefly affected by the minimum r-value [15]. The minimum r-values of both steels are nearly the same, and therefore the inferior hole expansion ratio of the Nb steel compared to the Ti steel cannot be explained from the viewpoint of the textural anisotropy.
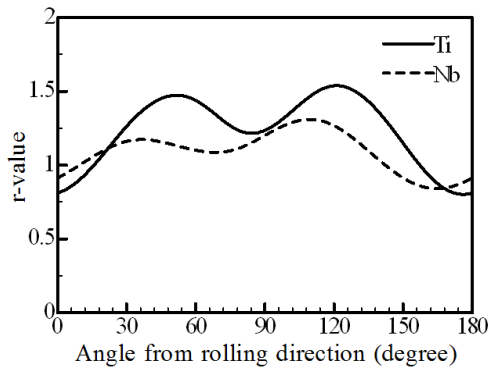
Figure 12. Planar anisotropy of r-values of Ti and Nb steels calculated with the orientation distribution function (ODF) data obtained by EBSP measurements.

At the bottom of the dimples in fractured surfaces, large precipitates were often observed. Figure 13 shows some results of the chemical composition of the precipitates in the Ti and Nb steels analysed by EDX. The precipitates analysed were $Ti_4C_2S_2$ and TiN in the Ti steel, and MnS and $NbCN$ in the Nb steel. Besides these large precipitates, there were numerous nano-size precipitates that contributed to the precipitation hardening.

Figure 13. Analysis of the chemical compositions of large precipitates
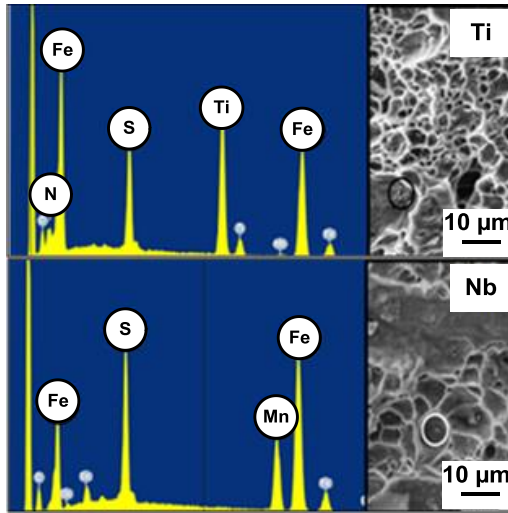found at the bottom of dimples.

Discussion

Table III shows a comparison of the experimental results of the Ti and Nb steels. The reason for the difference in the hole expansion ratio between the two steels is discussed by considering these results and the microstructural analyses.

Table III. Comparison of Experimental Results of Ti Steel and Nb Steel

	Ti	Nb
Ratio of sheared-to-fractured areas	59/39	46/49
Cracks observed during hole expansion	Many	Few
Micro-voids in the vicinity of pierced surface	Many	Few
Ferrite grain size	3.37 µm	2.27 µm
Dimple size	2.31 µm	3.62 µm
Micro-void size	1.4 µm	2.9 µm
Sulphide	$Ti_4C_2S_2$	MnS
Textural colonies	Not recognized	Present
Hardness at the pierced surface	310 HV	295 HV

As seen in Figure 6, the fraction of the fractured area of the pierced surface of the Nb steel was markedly higher than that of the Ti steel. It is understandable that the high fraction of the fractured area of the pierced surface in the Nb steel has lowered hole expandability. The reason why the Nb steel has a high fraction of the fractured surface should be discussed. A high ratio of the fractured areas indicates that the Nb steel was more prone to fracture than the Ti steel. It is well known that grain refinement is effective for suppressing fracture. The measured mean ferrite grain size of the Nb steel was smaller than that of the Ti steel. This experimental finding led us to expect that the Nb steel would have the higher resistance to fracture, but this was not the case. This contradiction can be interpreted as follows. The resistance to fracture is enhanced by the existence of high angle boundaries, which hinder crack propagation. The formation of the textural colonies (with low angle boundaries) in the Nb steel meant a reduction in the effective grain boundary suppression of crack propagation. As a result, the effective grain size of the Nb steel increased, as indicated by the fact that the size of dimples and micro-voids of the Nb steel was large.

As seen in Figures 4 and 5, there were more cracks in the Ti steel than in the Nb steel, and there were also more micro-voids formed by piercing in the Ti steel than in the Nb steel. The higher sensitivity to crack initiation in the Ti steel may be caused by the existence of rectangular-shaped large TiN. The initiation of many cracks in the pierced surface during hole expansion contributes to stress release at the tip of the crack, and this release is supposed to suppress propagation of through-thickness cracks in Ti steel.

In the Ti steel, cracks were observed over the entire circumference of the pierced surface during hole expansion. In contrast, the cracks in the Nb steel were usually formed along the rolling direction, as seen in Figure 2. It is not obvious that the hole expansion ratio has a close relationship with toughness. However, Takahashi et al. [16] indicated a certain relationship between the hole expansion ratio and toughness by revealing a tight correlation of the hole expansion ratio with the Jc value. Therefore, the reason that the through-thickness cracks of the Nb steel are restrictedly formed in the direction parallel to rolling is discussed with the result of the Charpy impact test. As seen in Table II, the Nb steel has a large planar anisotropy of impact energy, and the impact energy in the direction parallel to rolling is significantly lower. The low impact energy parallel to the rolling direction is inferred to be caused by the existence of elongated large textural colonies and flattened ("pancaked") MnS.

It is well known that the presence of MnS deformed by rolling lowers hole expandability. To examine the quantitative influence of MnS on the hole expansion ratio, a steel was produced by adding 0.0074%Ca to the Nb steel. By addition of Ca, the sulphide formed in the Nb steel became CaS instead of MnS. CaS is hard, and is not pancaked by hot-rolling. The formation of the so-called 'shape-controlled sulphide' was expected to improve the hole expansion ratio. Through this measure, the hole expansion ratio improved from 96% to 113% for the pierced specimens and from 187% to 202% for the machined specimens, respectively. There is still a clear difference in the strength–ductility–hole expansion ratio balance between the Nb and Ti steels. This result indicates that a large amount of the Nb addition itself detrimentally affects hole expandability. Because the quantity and size of NbC in the Nb steel and TiC in the Ti steel hardly differ from each other, the detrimental effect of Nb is inferred to be mainly caused by the formation of the heterogeneous microstructure with elongated, large textural colonies.

From these considerations, the suppression of the formation of large textural colonies and MnS seems to be important to achieve a good strength–ductility–hole expansion ratio balance in steel consisting of a ferrite matrix strengthened by finely dispersed precipitates. Since we supposed that a moderate addition of Nb would result in grain refinement without forming textural colonies, and could improve hole expandability, we carried out an additional experiment using a steel based on the Ti steel with moderate addition of Nb (hereafter called Ti–Nb steel). A small amount of Ti in the Ti steel was substituted by Nb. Table IV shows the chemical composition of the Ti–Nb steel. Table V shows the mechanical properties of the Ti–Nb steel compared with those of the Ti steel and Nb steel. The strength–ductility–hole expansion ratio balance of the Ti–Nb steel was the best among the steels investigated. The sulphide in the Ti–Nb steel was exclusively $Ti_4C_2S_2$. Figure 14 shows the microstructure of the Ti–Nb steel. The large and elongated textural colonies observed in the Nb steel were hardly evident in the Ti–Nb steel, and the mean ferrite grain size was 2.87 µm which is smaller than that of Ti steel.

Table IV. Chemical Composition of Ti–Nb Steel (wt%)

Steel	C	Si	Mn	P	S	Al	Nb	Ti	N
Ti-Nb	0.035	0.1	1.46	0.0048	0.0057	0.038	0.021	0.112	0.0029

Table V. Mechanical Properties of Ti Steel, Ti-Nb Steel and Nb Steel

	TS (MPa)	T.El (%)	U.El (%)	L.El (%)	λ (%)	TS×El×λ (MPa %^{2})
Ti	604	19.8	10.6	9.2	140	1674288
Ti-Nb	607	20.9	11.2	9.7	151	1915631
Nb	575	18.2	10.9	7.3	96	1004640

This result supported the conclusion that the inferior strength–ductility–hole expansion ratio balance in the Nb steel was caused by the formation of large and elongated textural colonies and deformable sulphide, and that the strength–ductility–hole expansion ratio balance of the Ti steel can be improved by proper addition of Nb, which refines the ferrite microstructure without formation of textural colonies.
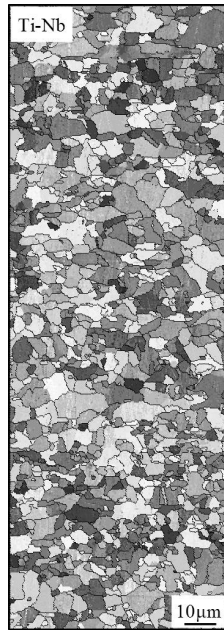
Figure 14. ND crystal orientation map of Ti-Nb steel.

Conclusions

1. An alloy composition incorporating a carefully balanced combination of Nb and Ti has been shown to provide a favourable combination of properties including the required strength-ductility-hole expansion ratio balance.

2. The enhanced properties have been achieved by optimum strengthening of the ferrite matrix by a large volume of finely dispersed precipitates as well as grain refinement.

3. Neither Ti nor Nb on its own, within the experimental composition limits studied, was capable of providing the best result.

4. Ti-only microalloyed steel resulted in a higher shear area at the edge of a punched hole and exhibited many microcracks over the entire circumference after hole expansion. However these cracks were not growing into a macroscopic crack.

5. Nb-only microalloyed steel resulted in a smaller shear area at the edge of a punched hole and exhibited fewer microcracks, which however propagated into macroscopic cracks at a smaller hole expansion ratio.

6. The ferrite grain size of the Nb steel was finer than that of the Ti steel but the former also contained large textural colonies. Such textural colonies can provide an easy crack path and may lead to larger dimples on the fracture surface compared to the Ti steel.

7. MnS and NbCN particles were observed in the fracture dimples of the Nb steel, whereas in the Ti steel TiN and $Ti_4C_2S_2$ particles were primarily observed.

8. The size and volume fraction of precipitates in the two steels (Nb and Ti alone) were similar.

9. It is postulated that larger textural colonies and the presence of deformable MnS may have been responsible for the poorer strength-ductility–hole expansion ratio in the first Nb steel studied.

10. A dual Ti+Nb microalloyed steel using a Nb level providing efficient grain refinement but avoiding the formation of textural colonies appears to deliver the optimum combination of properties.

Acknowledgements

References

1. S. Hayami and T. Furukawa (Paper presented at the Micro Alloying '75 Symposium on High-strength, Low-alloy Steels, Products and Process, Washington, D.C. 1975), 59.

2. O. Matsumura, Y. Sakuma, and H. Takechi, "Enhancement of Elongation by Retained Austenite in Intercritical Annealed 0.4 C - 1.5 Si - 0.8Mn Steel," *Transactions of the Iron and Steel Institute of Japan,* 27 (7) (1987), 570-579.

3. K. Sugimoto et al., "Retained Austenite Characteristics and Tensile Properties in a TRIP Type Bainitic Sheet Steel," *Iron and Steel Institute of Japan International*, 40 (9) (2000), 902-908.

4. K. Sugimoto et al., "Ductility and Formability of Newly Developed High Strength Low Alloy TRIP-aided Sheet Steels with Annealed Martensite Matrix," *Iron and Steel Institute of Japan International*, 42 (8) (2002), 910-915.

5. Y. Funakawa et al., "Development of High Strength Hot-rolled Sheet Steel Consisting of Ferrite and Nanometer-sized Carbides," *Iron and Steel Institute of Japan International*, 44 (11) (2004), 1945-1951.

6. M. Morita et al., "Development of Hot-rolled High Strength Steels Hardened by Precipitation Hardening with High Stretch Flanging," *CAMP - Iron and Steel Institute of Japan International,* 5 (1992), 1863.

7. M. Morita et al., "Development of Precipitation Hardened Ferrite and Martensite Dual Phase Steel for Automotive Wheel," *Materia Japan*, 37 (6) (1998), 513-515.

8. Y. Mukai, "Development of New High-strength Steel Sheets for Automobiles," *Kobe Seikou Giho*, 55 (2) (2005), 30.

9. T. Nonaka et al., "Developments of Ultra High-strength Cold-rolled Steel Sheets for Automotive Use," *Shinnittetsu Giho*, 378 (2003), 12-14.

10. T. Tsumashika, K. Hasegawa, and H. Kawabe, "Ultra High-strength Steel Sheets Leading to Great Improvement in Crashworthiness," *JFE Giho*, 4 (2004), 33.

11. Y. Omiya, "Developments and Trends Related to High-strength Steel Sheet for Automotive Use," *Kobe Seikou Giho*, 50 (2000), 20.

12. N. Yoshinaga, "Symposium on Materials for Automobiles," (2006), 15, (ISIJ).

13. T. Kashima and Y. Mukai, "Materials for Automotive Industry: Development of 780 MPa Class High Strength Hot Rolled Steel Sheet with Super High Flange Formability," *Kobe Steel Engineering Reports*, 52 (3) (2002), 19-22.

14. Y. Funakawa and K. Seto, "Stabilization in Strength of Hot-rolled Sheet Steel Strengthened by Nanometer-sized Carbides," *Tetsu-to-Hagane (Journal of the Iron and Steel Institute of Japan)*, 93 (1) (2007), 49-56.

15. A. Phillips et al., "Effect of Microstructure and Texture on the Edge Formability of Light Gauge Strip Steel," *Iron and Steel Institute of Japan International*, 51 (5) (2011), 832-842.

16. Y. Takahashi et al., "Fracture Mechanical Study on Edge Flangebility of High Tensile-strength Steel Sheets," *Proceedings of the Materials Science and Technology Conference 2009*, Pittsburgh, USA, (25-29 October 2009), 1317-1402.